PROCEEDINGS OF SCIENCE

Analysis of cosmic lithium, beryllium and boron with the DAMPE space mission

Andrea Parenti,[a,b,*] **Zhan-Fang Chen,**[c,d] **Ivan De Mitri,**[a,b] **Mikhail Stolpovskiy,**[e] **Li-Bo Wu**[a,b,**] **and En-Heng Xu**[f] **on behalf of the DAMPE collaboration**

[a] *Gran Sasso Science Institute (GSSI), Via Iacobucci 2, L'Aquila, Italy*

[b] *Istituto Nazionale di Fisica Nucleare (INFN) - Laboratori Nazionali del Gran Sasso, Assergi, L'Aquila, Italy*

[c] *Key Laboratory of Dark Matter and Space Astronomy, Purple Mountain Observatory, Chinese Academy of Sciences, Nanjing, China*

[d] *School of Astronomy and Space Science, University of Science and Technology of China, Hefei, China*

[e] *Department of Nuclear and Particle Physics, University of Geneva, Geneva, Switzerland*

[f] *Department of Modern Physics, University of Science and Technology of China Hefei, China*

[**] *now at Institute of Deep Space Sciences, Deep Space Exploration Laboratory, Hefei, China*

E-mail: andrea.parenti@gssi.it

DAMPE (DArk Matter Particle Explorer) is a space-based particle detector that has been continuously taking data since its successful launch in December 2015. Its primary scientific goals include the indirect search of dark matter, the study of galactic cosmic rays with energy from few tens of GeV up to hundreds of TeV and high-energy gamma-ray astronomy. Spectral measurements of secondary nuclei such as lithium, beryllium and boron and ratios to primary fluxes are fundamental to improve our understanding of cosmic ray acceleration and propagation. In this work, first preliminary results on DAMPE data analysis of these elements will be presented.

38th International Cosmic Ray Conference (ICRC2023)
26 July - 3 August, 2023
Nagoya, Japan

ICRC2023
38th International Cosmic Ray Conference
The Astroparticle Physics Conference

[*] Speaker

PoS(ICRC2023)137

1. Introduction

Galactic Cosmic Rays (GCRs) are high energy particles that are accelerated and travel through our Galaxy, constituting a unique probe for their sources and the Interstellar Medium (ISM) that they cross. Cosmic lithium, beryllium and boron are produced by spallation of heavier nuclei with the ISM and are therefore called secondary cosmic rays. Their stellar nucleosynthesis production abundances are orders of magnitude lower than protons, helium, carbon and oxygen, which are referred to as primary cosmic rays. Measurements of lithium, beryllium and boron fluxes by AMS-02 [1, 2] in the 1.9 GV - 3.3 TV rigidity range have shown a hardening of the spectral index in their spectra above 200 GV. The DAMPE experiment recently measured the B/C and B/O ratios [3], fundamental to probe the CR diffusion mechanisms, reporting a hardening at 100 GeV/n in both ratios with high significance, strongly reinforcing the hypothesis of such feature being a propagation related effect. Precision measurements of the secondary cosmic rays are now therefore fundamental to investigate this feature and gain a better understanding of CR propagation. This work will show preliminary measurements of cosmic lithium, beryllium and boron DAMPE detector.

2. The DAMPE detector

The Dark Matter Particle Explorer (DAMPE) is a space-based CR detector that has been smoothly operational since its launch in December 2015. The instrument includes three main sub-detectors: a plastic scintillator (PSD), designed to measure the absolute value of the charge of the incoming particles and identify gamma-rays; a silicon-tungsten tracker-converter (STK) to measure the particles direction while also providing additional information on their charge; a very deep (32 X_O) bismuth germanium oxide electromagnetic calorimeter (BGO) to measure the energy of the particles and to distinguish hadronic and electromagnetic showers. For a full description of the instrumental apparatus, see Ref. [4]. DAMPE is a powerful CR telescope, capable of detecting electrons/positrons in an energy range of 10 GeV - 10 TeV and CR nuclei up to several hundreds of TeV.

3. Data and Monte-Carlo samples

The analysis presented is this work was performed using 72 months of data collected by the experiment in orbit, from January 2016 to December 2021. The events collected in the South Atlantic Anomaly have been discarded. Taking into account the time spent in the SAA along the DAMPE orbit, the instrumental dead-time and the time dedicated to the on-orbit calibration, the total exposure time is 1.44×10^8 s corresponding to $\sim$ 75.85% of the total operation time. Extensive Monte-Carlo (MC) simulations are also performed with the GEANT4 4.10.5 software toolkit adopting the FTFP_BERT and EPOS-LHC physics lists for simulations of the three nuclei in the 10 GeV - 500 TeV, linking GEANT4 with the Cosmic Ray Monte Carlo (CRMC) package [5]. The events are initially generated from an isotropic source around the detector, following a $E^{-1.0}$ spectral shape, and then re-weighted during the analysis to a $E^{-3.0}$ power-law. Different isotopes are simulated, namely Li6, Li7, Be7, Be9, Be10, B10 and B11. A weight can then be assigned to the simulation samples, corresponding to specific isotopic fractions. The following values have

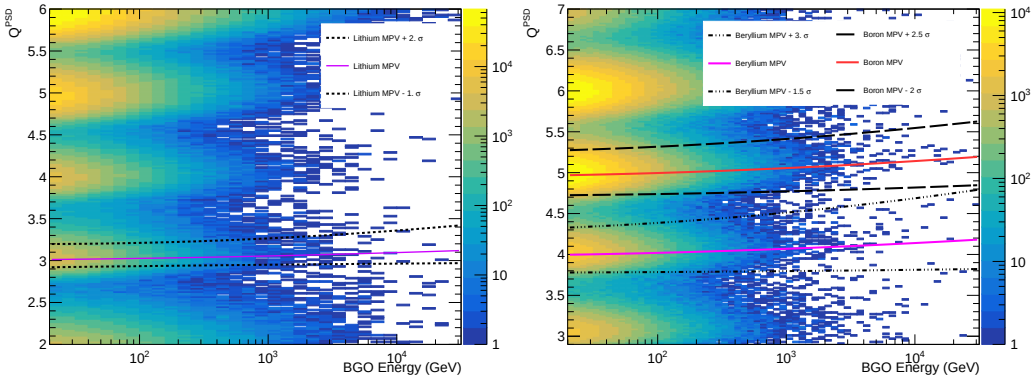

(a) **(b)**

Figure 1: Charge selection regions defined for the three nuclei as a function of the energy released in the BGO calorimeter. Regions for Boron and Beryllium are displayed together in Fig.1b, while Lithium which has a different sample pre-selection is shown in Fig.1a.

been chosen as a benchmark: Li6:Li7 = 1:1, Be7:Be9 = 1:1 and B10:B11 = 3:7. This fraction is then varied to evaluate the corresponding systematic effect on the measurements.

4. Event Selection

A common pre-selection is applied to the full data sample to ensure good quality data with properly reconstructed events in the detector. A selection tailored to the specific nucleus (Li, Be or B) follows.

4.1 Pre-selection

The pre-selection is a set of common requests for all of the three nuclei treated in this study, mainly involving the BGO calorimeter. Firstly, events must have a deposited BGO energy E_{BGO} larger than 80 (60) GeV for the Be,B (Li) analysis, to avoid the geomagnetic rigidity cutoff effect. Then several conditions involving the BGO energy deposit are required. The aim is to reject events entering from the side, select ones with optimal shower development and match the BGO track to other detectors. A track reconstruction algorithm identifies the best candidate track in the STK for each event, requesting at least one cluster in the first STK layer. The STK track is matched to the signal in the PSD and to the track in the BGO. Finally, events passing the High Energy Trigger (HET) are selected for this analysis (for the definition see [6]). The energy deposit in the first layer of the STK is used to reduce the contamination from other elements. Specifically, the signal in the first STK plane, for both X and Y layers, is requested to be larger than 600 ADC to remove a large portion of the proton and helium events in the Be, B analyses. For Li the threshold on the STK signal is instead set to 400 ADC.

4.2 Charge selection

The nuclei of interest are selected according to the signal in the PSD. The detector is made of four sub-layers, two oriented in the Y and two in the X direction. Due to this configuration,

every incoming particle can deposit energy in a different set of sub-layers according to its incoming direction and instrumental effects. At pre-selection stage events events are required to have a signal in at least one PSD X and one PSD Y layer. A PSD estimator of the particle charge is defined as:

$$Q^{PSD} = \frac{\sum_i Q_i^{PSD}}{N_{\text{lay}}} \tag{1}$$

where the index i goes over the PSD sub-layers with non-zero signal, checking that charges in successive sub-layers satisfy the condition:

$$|Q_i^{PSD} - Q_{i+1}^{PSD}| < Q_{th} \tag{2}$$

with a $Q_{th} = 1$ threshold choice for Be, B while a more stringent request of $Q_{th} = 0.3$ is adopted for Li. N_{lay} is the number of sub-layers passing this request. The PSD charge is defined is this way to improve the charge resolution by rejecting most events in which the incoming particle undergoes an inelastic interaction inside the PSD.
The Q^{PSD} variable retains a dependence on the primary energy, and therefore on the energy reconstructed in the BGO calorimeter. This has to be taken into account when choosing the signal region in terms of PSD charge. To understand its behaviour with energy, the PSD charge peak of the nucleus of interest is fitted with a convolution of a Landau and a Gaussian distribution for different E_{BGO} bins, from which the Most Probable Value (MPV) and the width σ, defined as:

$$\sigma = \sqrt{\sigma_{Gaus}^2 + \sigma_{Landau}^2} \tag{3}$$

are extracted. The dependence of MPV and σ on E_{BGO} are modeled with log-polynomial functions $f_{MPV}(E_{BGO})$ and $f_\sigma(E_{BGO})$ used to define an energy-dependent PSD charge selection window. The selected signal region is:

$$f_{MPV} - n_\sigma^{low} \cdot f_\sigma < Q^{PSD} < f_{MPV} - n_\sigma^{hi} \cdot f_\sigma \tag{4}$$

The Q^{PSD} signal window is chosen as a balance between high statistics and low background contamination. Each nucleus will have its specific functions f_{MPV} and f_σ. The chosen signal windows are $(n_\sigma^{low}, n_\sigma^{hi}) = (1, 2), (1.5, 3), (2, 2.5)$ for Li, Be and B respectively.

5. Background contamination

Background contamination from different nuclear species has to be carefully evaluated. A MC-based template fit is performed on the Q^{PSD} variable to estimate the background in the selected region for Li, Be or B. The reconstructed Q^{PSD} values for MC and data do not agree perfectly, probably due to backscattering particles which are not well modeled in the simulation. For this reason the MC Q^{PSD} is corrected with a so called "smearing" procedure, bringing it to a satisfying agreement with the data (for more details see [7, 8]). After the smearing has been performed, Q^{PSD} templates from MC simulations of all nuclei from protons up to oxygen are used to fit the data (see Fig. 2). For the boron sample selection, the background is well below 10% in the explored E_{BGO} range and is therefore considered under control. The associated systematic uncertainty is

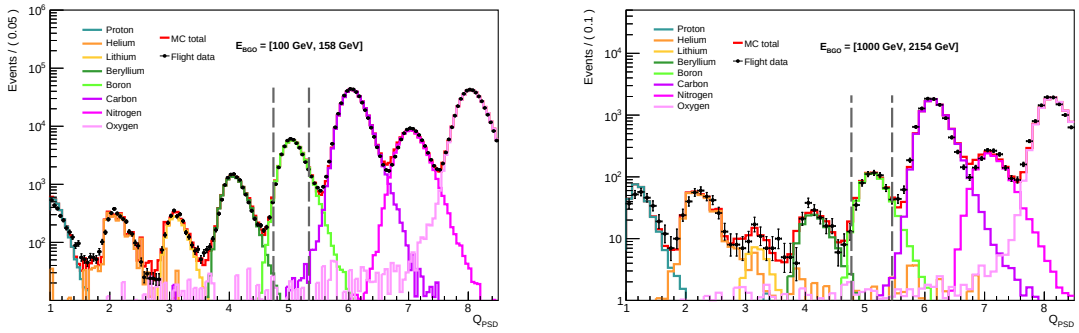

(a) **(b)**

Figure 2: MC-based template fit for E_{BGO} energy bin of $[100, 158]$ GeV (2a) and $[1, 2.2]$ TeV (2b) for the Boron analysis after all the pre-selection cuts. The black dots represent the flight data while the red line the best fit for the total MC model. The vertical gray dashed lines represent the chosen signal region.

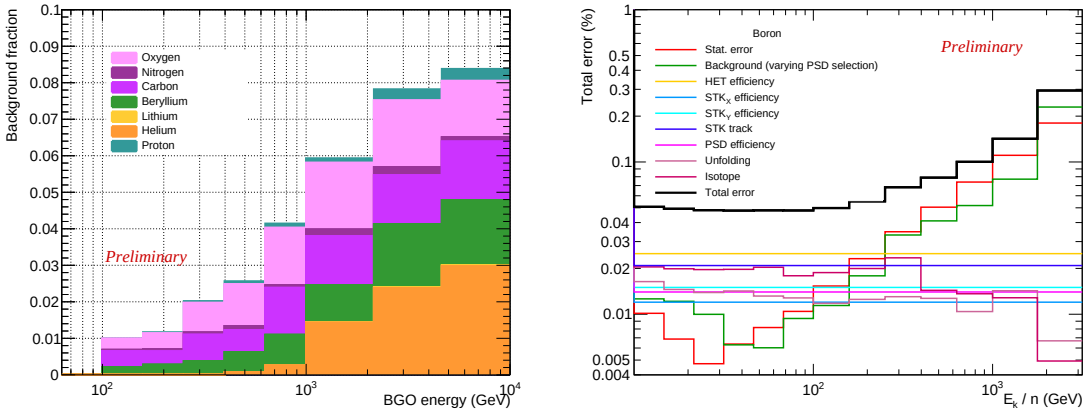

(a) **(b)**

Figure 3: Total background for boron analysis shown as a stack of the various components as a function of E_{BGO} (Fig. 3a). Fig 3b shows total uncertainty on the preliminary boron spectrum including statistical one (red) and the systematic contributions.

evaluated by shifting the PSD charge selection window to narrower or wider choices, and looking at the relative shift in the flux. For lithium and beryllium instead the background is much larger and strategies to further reduce it are currently under investigation. For these two analyses a background subtraction procedure is employed, reducing the observed counts as a function of E_{BGO} by the estimated fraction of background events.

6. Unfolding

An energy measurement of the event is provided by the BGO calorimeter, to which corrections to take into account for saturation and quenching effects in the detector are applied [9, 10]. Since the BGO calorimeter is 1.6 interaction lengths deep, it is not able to fully contain the hadronic showers

developed by CR nuclei. The energy deposited in the calorimeter will only be a fraction of its primary energy, subject to large fluctuations. The primary energy is reconstructed with a bayesian iterative unfolding procedure [11]. The number of events in the $j-$th bin of observed BGO energy, $N(E^j_{BGO})$ is related to the number of events in the $i-$th bin of true primary energy N_i by:

$$N_i = \sum_{j=1}^{n} P(E^i_T|E^j_{BGO})N(E^j_{BGO}) \tag{5}$$

where $P(E^i_T|E^j_{BGO})$ is the unfolding matrix computed starting from MC simulation through the unfolding technique.

7. Preliminary results

Once the full sample selection is defined and the background contamination estimated, the overall effective acceptance can be estimated from MC simulation. It is evaluated as:

$$\mathrm{A_i} = \mathrm{G_{gen}} \times \frac{\mathrm{N_{sel}(E^i_T)}}{\mathrm{N_{gen}(E^i_T)}} \tag{6}$$

where $\mathrm{G_{gen}}$ is the geometrical factor of the generated MC sample, $\mathrm{N_{gen}(E^i_T)}$ is the number of generated MC events in the i-th bin of primary energy $\mathrm{E_T}$, and $\mathrm{N_{sel}(E^i_T)}$ the number of MC events passing the full selection in the i-th bin of primary energy. The differential flux for each energy bin Φ_i is:

$$\Phi_\mathrm{i} = \frac{\mathrm{N_i}}{\Delta\mathrm{T} \times \mathrm{A_i} \times \Delta\mathrm{E_i}} \tag{7}$$

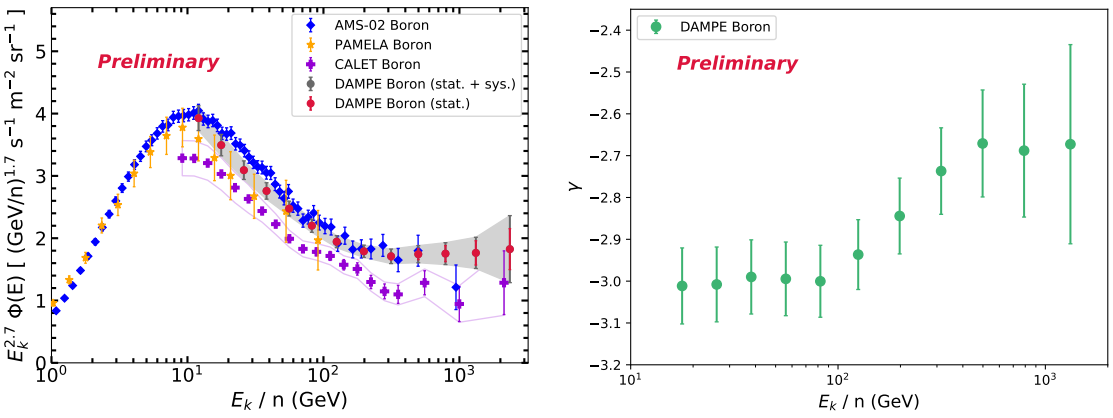

(a) **(b)**

Figure 4: Fig. 4a shows the preliminary boron spectrum measured with the DAMPE detector (red points) compared to PAMELA [12], AMS-02 [2] and CALET results [13]. The gray band shows the sum in quadrature of statistical and systematic uncertainties; the one related to the choice of hadronic model is not yet included and is under evaluation. Estimated spectral indexes from the sliding window power law fit are shown in Fig. 4b.

where N_i is the number of events in the i-th energy bin after the unfolding, ΔT the total exposure time, A_i the acceptance in the i-th bin, and ΔE_i the width of the i-th energy interval. Many sources of systematic uncertainties have been evaluated including efficiencies on the analysis cuts, choice of isotopic abundances, unfolding procedure, background contamination. The total error budget is shown is Fig. 3b. The boron spectrum was measured in the 10 GeV/n to 3.2 TeV/n energy range (see Fig. 4a) assuming a nucleon number of n(B) = 10.7. A fit with a power law $f(E_k) = AE_k^{\gamma}$ was performed in sliding windows of three points across the boron spectrum. The estimated spectral index as a function of the energy per nucleon is shown in Fig. 4b, featuring a hardening at a few hundred GeV per nucleon. The analysis is still ongoing to perfect the final steps, in particular the uncertainty from the hadronic model is currently being evaluated.

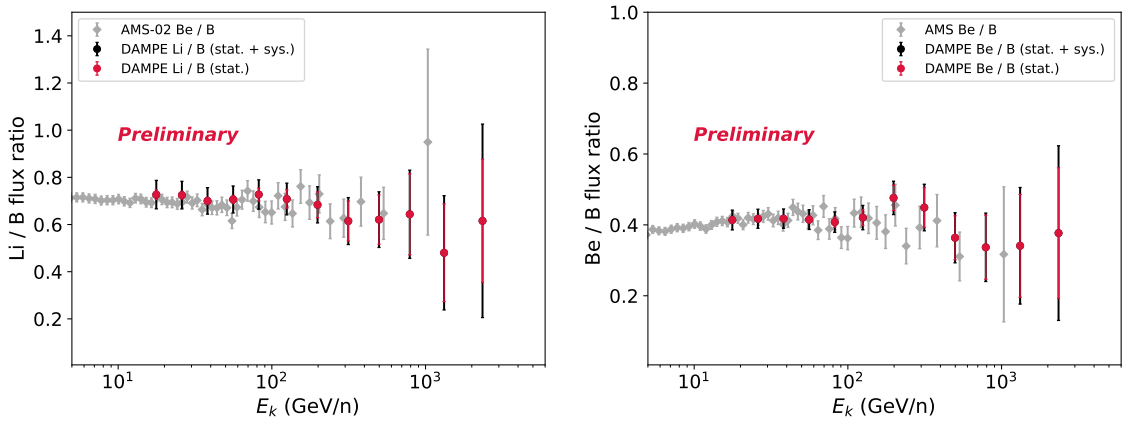

(a) **(b)**

Figure 5: Preliminary DAMPE Li/B (Fig. 5a), Be/B (Fig. 5b) ratios with statistical error (red) and a preliminary estimation of the systematic uncertainties plotted with results from AMS-02 [1]. Gray error bars represent the sum in quadrature of the statistical and systematic contributions.

A preliminary look at Li/B and Be/B ratios is shown in Fig. 5 from 14.7 GeV/n to 3.2 TeV/n with a preliminary estimation of the systematic uncertainties. The kinetic energy per nucleon was computed assuming n(Li) = 6.5 and n(Be) = 8. The analysis of the spectra of lithium and beryllium and their ratios is still ongoing, focusing on further reduction of the background and a complete evaluation of the systematic uncertainties.

Acknowledgments

The DAMPE mission was funded by the strategic priority science and technology projects in space science of Chinese Academy of Sciences (CAS). In China, the data analysis was supported by the National Key Research and Development Program of China (No. 2022YFF0503302) and the National Natural Science Foundation of China (Nos. 12103094, 12220101003, 11921003, 11903084, 12003076 and 12022503), the CAS Project for Young Scientists in Basic Research (No. YSBR061), the Youth Innovation Promotion Association of CAS, the Young Elite Scientists Sponsorship Program by CAST (No. YESS20220197), and the Program for Innovative Talents and Entrepreneur in Jiangsu. In Europe, the activities and data analysis are supported by the Swiss National Science Foundation (SNSF), Switzerland, the National Institute for Nuclear Physics (INFN), Italy, and the European Research Council (ERC) under the European Union's Horizon 2020 research and innovation programme (No. 851103).

References

[1] AMS collaboration, *Observation of new properties of secondary cosmic rays lithium, beryllium, and boron by the Alpha Magnetic Spectrometer on the international space station*, *Phys. Rev. Lett.* **120** (2018) 021101.

[2] AMS collaboration, *The Alpha Magnetic Spectrometer (AMS) on the international space station: Part ii — results from the first seven years*, *Physics Reports* **894** (2021) 1.

[3] DAMPE collaboration, *Detection of spectral hardenings in cosmic-ray boron-to-carbon and boron-to-oxygen flux ratios with DAMPE*, *Science Bulletin* **67** (2022) 2162.

[4] DAMPE collaboration, *The DArk Matter Particle Explorer mission*, *Astropart. Phys.* **95** (2017) 6 [1706.08453].

[5] A. Tykhonov, D. Droz, C. Yue, M. Cui et al., *TeV–PeV hadronic simulations with DAMPE*, *PoS* **ICRC2019** (2019) 143.

[6] Y.-Q. Zhang, J.-H. Guo, Y. Liu, C.-Q. Feng et al., *Design and on-orbit status of the trigger system for the DAMPE mission*, *Research in Astronomy and Astrophysics* **19** (2019) 123.

[7] DAMPE collaboration, *Measurement of the cosmic ray proton spectrum from 40 GeV to 100 TeV with the DAMPE satellite*, *Science Advances* **5** (2019) eaax3793.

[8] DAMPE collaboration, *Measurement of the cosmic ray helium energy spectrum from 70 GeV to 80 TeV with the DAMPE space mission*, *Phys. Rev. Lett.* **126** (2021) 201102.

[9] C. Yue, P.-X. Ma, M.D. Santo, L.-B. Wu et al., *Correction method for the readout saturation of the DAMPE calorimeter*, *NIM-A* **984** (2020) 164645.

[10] Y. Wei, Y. Zhang, Z. Zhang, L. Wu et al., *The quenching effect of BGO crystals on relativistic heavy ions in the DAMPE experiment*, *IEEE Trans. Nucl.* **67** (2020) 939.

[11] G. D'Agostini, *A multidimensional unfolding method based on Bayes' theorem*, *NIM-A* **362** (1995) 487.

[12] O. Adriani, G.C. Barbarino, G.A. Bazilevskaya, R. Bellotti et al., *Measurement of boron and carbon fluxes in cosmic rays with the PAMELA experiment*, *The Astrophysical Journal* **791** (2014) 93.

[13] CALET collaboration, *Cosmic-ray boron flux measured from* 8.4 GeV/n *to* 3.8 TeV/n *with the calorimetric electron telescope on the international space station*, *Phys. Rev. Lett.* **129** (2022) 251103.